3DPPS for Early Detection of Arcing Faults

Dominik Bak, Seung-Jae Lee, Sang-Hee Kang, Myeon-Song Choi
Next Generation Power Technology Center
Myongji University
Yongin, Rep. of Korea

Waldemar Rebizant
Institute of Electrical Power Engineering
Wroclaw University of Technology
Poland

***Abstract*—New approach to high impedance fault detection, which allows for detecting it basing on yet some random arcing at the beginning of the fault, is presented in this paper. The proposed solution was developed within novel protection methodology—3D power protection scheme (3DPPS). The identification of the fault is based on monitoring of symmetry deviations of three phase voltage or current signals. Fundamental signal components carry the biggest amount of information on the actual state of the protected system and are processed in order to extract out the necessary information proving an occurrence of a high impedance fault that must be cleared for safety purposes.**

***Index Terms*—high impedance fault, distribution system, electrical arc, 3D power protection scheme**

I. Introduction

THE electric arc accompanies most cases of faults in medium voltage power system. It may occur not only during well developed faults but especially in the very first stage of a fault development when there is some random sparking. As it depends on material properties of an object at a fault place whether accidental flash-overs keep coming in a sparking fault or it would turn into a high impedance fault and later high current one. Both sparking fauls, because of stochastic nature, and high impedance ones, because of small fault current magnitude values, can still make difficulties in their detecting. Standard protection devices which must be set in order to allow for signal disturbances and phase currents' unbalancing usually fail to detect them until the current in the faulty line becomes high enough. As HIFs might remain undetected and not cleared out, they cause the danger of electric shock to accidental by-passers or a fire due to electric arc burning at a fault place. To prevent such hazardous situations HIFs call for separate protection schemes with dedicated to their recognition algorithms.

So far, proposals for HIF detection which are reported can be categorized as follows:

a) algorithms combining together unbalanced load currents and neutral one [1], as well as ground current [2], in order to construct a signal which is in proportion to a fault current;
b) methods based on analysis of electrical arc phenomena which usually accompany HIF at a fault place; the phase signals are first transformed into 012 signal components, decomposed into harmonics, which are next processed in order to extract out information indicating HIF occurrence.

Among them one can point out applications of the wavelet transformation against zero sequence component of voltage or current like proposed in [3], an approach with neural networks operating on zero sequence power as proposed in [5], a direction of a residual current [4], a measure of an incremental variance of an even order harmonic power [6], an analysis of energy variations in concerned frequency bands [7], current low frequency spectrum analysis [8], Kalman filtering technique for harmonics analysis in HIF signals [9], a fuzzy system and external impulse signal injected into feeder for HIF identification [10].

This paper presents new general methodology for HIF detection scheme developed by authors. It is a continuation of our former research presented in [11] and [12]. The paper addresses the possibility of sparking fault detection and the most important issues of new approach already presented in [11], which are to be briefly repeated to provide comprehensive integrity of presented ideas as well as the general organization of the scheme and especially its decision making part.

The following sections of the paper describe the model of an electrical arc and its interpretation for HIF detection purposes (Sec. II). The developed 3DPPS methodology for sparking and high impedance faults detection together with simulation results are given in Sec. III. Conclusions in Sec. IV close the paper. MV network model used for simulation purposes is presented in Appendix.

II. MV Electric Arc and its Role in HIF Detection

Faults in MV networks are mostly accompanied at a fault place by an electrical arc, which behavior fully determines the course of that fault.

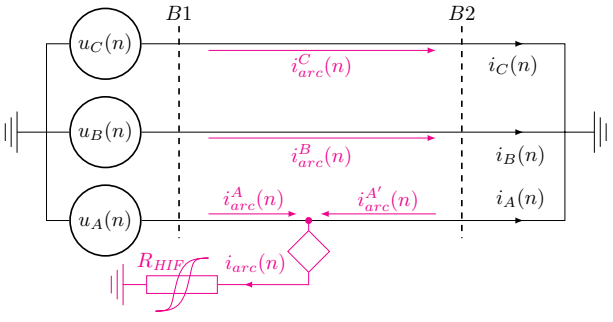

Fig. 1. Arc represented as a current source and a current flow at HIF

A simplified diagram of MV line with HIF is presented in Fig. 1. The nonlinear resistance R_{HIF} represents both arc resistance and connected in series some big resistance of a foreign object that takes part in a fault, e.g. a tree. An electrical arc at a fault place FP is represented as nonlinear current source $i_{arc}(t)$ controlled by arc voltage $u_{arc}(t)$ according to

$$i_{arc}(t) = g(t) \cdot u_{arc}(t) \tag{1}$$

where: $g(t)$ is arc conductance and can be calculated as in [3]

$$\frac{dg(t)}{dt} = \frac{G(t) - g(t)}{\tau} \tag{2}$$

$$G(t) = \frac{|i_{arc}(t)|}{(u'_{arc} + R'_{arc} \cdot |i_{arc}(t)|) \cdot l_{arc}} \tag{3}$$

where: $G(t)$ – stationary arc conductance, τ – time constant, u'_{arc} – constant voltage parameter per arc length, R'_{arc} – arc resistance per unit length and l_{arc} – arc length. The voltage $u_{arc}(t)$ is in phase with the phase voltage at a fault place U_{FP}.

As it was derived in [11], during HIF currents and voltages measured at a relay point at busbars $B1$ can be decomposed into two components, which have the same pulsation but different phases

$$i_A^{HIF}(t) = i_A(t) + i_{arc}^A \tag{4}$$

The fault current $i_{arc}^A(t)$ by means of electromagnetic couplings and even more by evoking changes of the voltage at the transformer neutral point on MV side affects voltage and current signals measured also in healthy phases by feeding in the components which are in phase with $i_{arc}^A(t)$.

Presented above very simplified new insight into HIF phenomenon indicates that, during that kind of events, measured signals of phase voltages and currents can be regarded as superimposed from two components of the same frequency but different in phase and amplitude (one of which is strongly nonlinear). The first component is associated with phase voltage or load current signal and considered as a set of three signals defining the actual current system symmetry. The second components

$$i_{arc}^A,\ i_{arc}^B \text{ and } i_{arc}^C \tag{5}$$

make up a set which describes system symmetry violations.

Newly developed HIF criterion quantity algorithm presented below not only removes the first set of signals but can also utilize it to exaggerate the signals of the second one to easily measurable level.

III. HIF Detection Methodology

A. Phase Signal Decomposition and Interpretation

A digital relay is provided with sampled phase signals of a voltage and/or current in which the fundamental component is often accompanied by higher harmonics $X_i(n)$, exponential components $X_e^T(n)$ with time constant T and all other distortions $d(n)$ of the signal, e.g. due to CT core saturation or in our case mostly to arc current

$$x(n) = X_{1m}\cos(2\pi f_1 n T_S + \varphi_1) + \sum_{i \neq 1} X_i(n) + \sum_T X_e^T(n) + d(n) \tag{6}$$

where: X_{1m}, f_1 and φ_1 are parameters of the fundamental component: amplitude, frequency and phase; T_S – sampling period. The phase signals carry all necessary information to differentiate load operation conditions from faulty ones but a relay considers and processes each signal separately (losing some part of information). That is the main difference between standard methods and 3DPPS which takes the advantage of the fact that a change of a signal in one phase affects two other phases and voltage or current phase signals can be arranged into one system of signals described by its external property—the signal system symmetry.

In the signal theory a three phase signal set is called symmetrical if amplitudes of all three signals are equal and phase shifts between each two successive signals is $\pm 2\pi/3$.

The components of the signal $x(n)$ in (6) can be divided into two groups. The first one associated with load conditions in a system—here we have fundamental component and harmonics which content is constant during a steady state of a system operation but can be changed after system moves from one steady state to another. The other group includes all transient disturbances and noises as well as arc current due to its nonlinearity. It is also assumed that in second group relative amount of all disturbances is constant during a sound steady state. As can be easily noticed the first group constitutes the system symmetry with fundamentals parameters

$$I_m^A = I_m^B = I_m^C = I \text{ and } \varphi_A = \varphi_B = \varphi_C = \varphi \tag{7}$$

and the other group houses all information on that system symmetry deviations.

Signals in a distribution system rarely meet the conditions (7); instead due to load unbalance and electromagnetic couplings they make more or less asymmetrical systems of signals with

$$I_m^A \neq I_m^B \neq I_m^C \text{ and } \varphi_A \neq \varphi_B \neq \varphi_C \tag{8}$$

Standard approach to deal with an asymmetrical system of signals is to transform it into 012 signal components. In proposed method we take advantage of alternative way of decomposing of an asymmetrical system of the signals (8) into two component sets: one which is symmetrical and the other which is not

$$\begin{cases} I_m^A = I_m^a + \Delta I_m^a \\ I_m^B = I_m^b + \Delta I_m^b \\ I_m^C = I_m^c + \Delta I_m^c \end{cases} \text{ and } \begin{cases} \varphi_A = \varphi_a + \Delta\varphi_a \\ \varphi_B = \varphi_b + \Delta\varphi_b \\ \varphi_C = \varphi_c + \Delta\varphi_c \end{cases} \tag{9}$$

The decomposition of asymmetrical signal set (8) into (9) results then in a virtual symmetrical signal set

$$I_m^a = I_m^b = I_m^c = I \text{ and } \varphi_a = \varphi_v = \varphi_c = \varphi \tag{10}$$

and the rest, which is asymmetrical

$$\Delta I_m^a \neq \Delta I_m^b \neq \Delta I_m^c \text{ and } \Delta\varphi_a \neq \Delta\varphi_v \neq \Delta\varphi_c \tag{11}$$

Current components (5) that appear during HIF fault all contribute to the virtual asymmetrical signal set (11). All signal disturbances and parts of load currents due to phase unbalance also feed into (11) and altogether with the symmetrical part

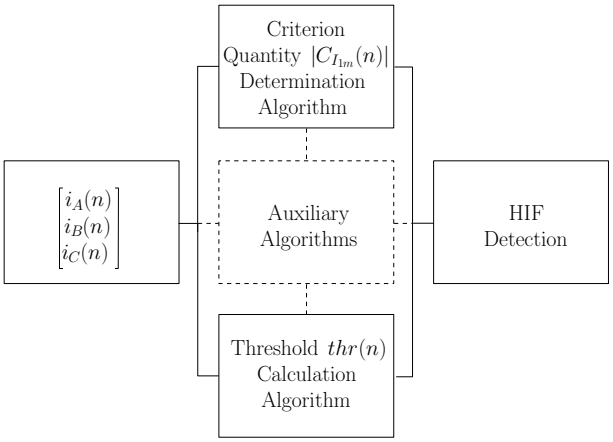

Fig. 2. HIF detection scheme diagram

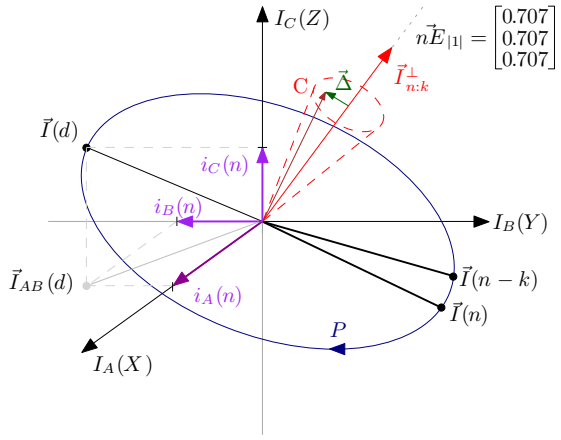

Fig. 3. Graphic presentation of 3D power protection scheme basic vectors and their construction

of the decomposition (9) given by (10) can be later removed while processing to attain a signal driven by arc current component (11) only.

B. HIF Detection Scheme General Structure

Standard protection schemes usually focus on a specific component of a signal (6) in order to differentiate sound and fault conditions in a system. Even if a signal which carries information to be extracted can be often quite small there always occurs loosing of some information on identified phenomena during signal processing. In presented HIF detection scheme another approach was applied, which makes it similar to adaptive algorithms. General HIF detection scheme diagram is shown in Fig. 2. Namely, there are two algorithms derived using different methodologies. Both algorithms process the same phase signal samples but in different ways. One determines a criterion quantity signal and, made within 3D Power Protection Scheme, was in detail described in [11]. The criterion quantity signal is computed that way in order to provide information on amount of disturbances of phase signals. It is especially oriented towards detecting the presence of arc current which, thanks to its nonlinearity (resulting from randomness), can be used to yield very strongly augmented signal that is also strongly correlated with arc current.

The other algorithm is used to set a threshold value. It is derived within standard signal processing methodology and aimed at delivering information on load current conditions. Values of both signals are further processed in HIF detection block to produce HIF alarm.

The auxiliary algorithms block in Fig. 2 houses optimization algorithms to enhance operation of presented HIF protection scheme. They are not describedin this paper.

C. 3D Power Protection Scheme Basics

The basic element in 3DPPS is *current (voltage) line vector* which is formed by assembling samples of a digitized phase signals into one three-dimensional space vector, where phase signals are considered as x, y and z vectors components

$$\begin{cases} i_A(n) = I_m^A \cos(n\omega T_S + \varphi_A) \\ i_B(n) = I_m^B \cos(n\omega T_S + \varphi_B) \\ i_C(n) = I_m^C \cos(n\omega T_S + \varphi_C) \end{cases} \rightarrow \vec{I}(n) = \begin{bmatrix} i_A(n) \\ i_B(n) \\ i_C(n) \end{bmatrix} \quad (12)$$

(see also Fig. 3 for illustration of $\vec{I}(n)$).

During steady state system operation *the current line vector* travels in 3D space, its end stretches a path being a closed curve. If current phase signals (12) are symmetrical, according to (7), then the closed curve P is a circle, otherwise it is an ellipse. As *the current line vector* is non-stationary, it rotates and can be transformed by a vector product of *current line vectors* taken at different time instances $\vec{I}(n)$ and $\vec{I}(n-k)$ into *a stationary current purpendicular-to vector*

$$\vec{I}^{\perp}_{n:k} = \vec{I}(n) \times \vec{I}(n-k) = \begin{vmatrix} x & y & z \\ i_A(n) & i_B(n) & i_C(n) \\ i_A(n-k) & i_B(n-k) & i_C(n-k) \end{vmatrix} \quad (13)$$

D. 3D HIF Criterion Quantity Signal Algorithm

Hereby the algorithim how to process the phase current signals into the criterion quantity will be briefly introduced, for detailed descreption of each transformation refer to [11].

The very first step is to calculate *the current perpendicular-to vector* (13) from *line current vectors* (12) with a delay parameter $k = N_1/3$ in order to remove the third harmonic multiples from phase current signals at the very beginning. Next the components of (13) are treated with mean filter and two orthogonal vectors are calculated. The first one

$$\Sigma^{\downarrow} \vec{I}^{\perp}_{n:k} = \begin{bmatrix} I^{\perp}_{n:k}(y) + I^{\perp}_{n:k}(z) \\ I^{\perp}_{n:k}(z) + I^{\perp}_{n:k}(x) \\ I^{\perp}_{n:k}(x) + I^{\perp}_{n:k}(y) \end{bmatrix} \quad (14)$$

is a function of a magnitude of symmetrical set signals (10) and provides rough information on current changes and therefore is named *a current perpendicular-to trend vector*. The transformation (14) can be also regarded as a vector structural averaging. The second one, which can be recognized

as a structural derivative of a vector cumulates information on disturbances and is called *current perpendicular-to detail vector*

$$\Delta^{\downarrow}\vec{I}^{\perp}_{n:k} = \begin{bmatrix} I^{\perp}_{n:k}(y) - I^{\perp}_{n:k}(z) \\ I^{\perp}_{n:k}(z) - I^{\perp}_{n:k}(x) \\ I^{\perp}_{n:k}(x) - I^{\perp}_{n:k}(y) \end{bmatrix} \tag{15}$$

which is a function of all signal disturbances (11). Then combining (14) and (15) according to (16) yields *a current leverage vector*, which next can be turn by transformation (17) with a delay parameter $d = N_1/4$ into *a current error-driven vector*. Coordinates of the vector (17) are combined together into, strongly correlated with arc current, *a current error driven signal* given by formula (18).

$$\vec{I}^{\otimes}_{n:k} = \Delta^{\downarrow}\vec{I}^{\perp}_{n:k} \times \Sigma^{\downarrow}\vec{I}^{\perp}_{n:k} \tag{16}$$

$$\vec{I}^{\times}_{n:d:k} = \vec{I}^{\otimes}_{n:k} \times \vec{I}^{\otimes}_{n-d:k} \tag{17}$$

$$C_I(n) = \frac{\sum_i \vec{I}^{\times}_{n:d:k}(i)}{3 \cdot \sum_i \left(\vec{I}^{\perp}_{n:k}(i)\right)^2} \tag{18}$$

It can be seen that if there are no disturbances in phase signals all coordinates in (13) are equal and (15) becomes zero what results in zeroing later on a criterion quantity signal $|C_I(n)|$.

Estimates of the amplitude of the fundamental component of (18) determine the *HIF 3D criterion quantity signal* $|C_{I_{1m}}(n)|$. Standard $\sin$ $\cos$ orthogonal filters and Fourrier algorithm of square root of sum of squares is used for that purpose.

E. Threshold Setting Algorithm

That algorithm is to provide information on amount of symmetrical part of phase signal decomposition (10). It is made using standard averaging algorithms in order to attenuate accompanying disturbances as much as possible.

The threshold value calculation starts with obtaining RMS magnitudes of phase currents to compute *a line base current signal*, which can be set as

$$I_{LB}(n) = \frac{I_A(n) + I_B(n) + I_C(n)}{3} \tag{19}$$

The threshold value $thr(n)$ is a function of *the line base current signal*. It can be a linear function if there are only very small disturbances in phase signals but generally it is a nonlinear one. A fourth order polynomial serves well the purpose

$$thr(n) = \sum_{k=1}^{4} a_k \cdot (I_{LB})^k \tag{20}$$

where coefficients a_k are functions of phase noise magnitude which are determined by auxiliary algorithms or in case if noise magnitudes are constant in a system then coefficients a_k can be calculated once and set as constant values. Threshold values (20) do not have to be calculated at every sampling cycle.

F. HIF Decision Making Scheme

HIF alarm signal which is formed as a difference of *the criterion quantity* and *threshold signals*

$$A_{HIF}(n) = C_{I_{1m}}(n) - thr(n) \tag{21}$$

is used for HIF decision making purpose. In fact, it is only a sign of values (21) which matters. Negative values refer to normal load conditions and positive ones indicate a fault. However in case when a feeder or a big load is switched on or off the *HIF alarm signal* can become positive during operational transients which last up to about two periods of the phase signal fundamental, therefore *a safety margin delay* is introduced to prevent false signaling and switching off a feeder. *The safety margin delay* is also longer than transient state induced by single flash-over. HIF is detected if

- *the HIF alarm signal* stays positive for more than *the safety margin delay*—the desicion to switch off a feeder is issued or
- there is more flash-overs counted within a set period than a-priori assumed *sparking fault count limit*—sparking fault detection signal is activated.

Examples of *HIF alarm signal* time history for faulty and sound feeders are plotted in Fig. 4. The sound feeder is connected to busbars all the time while the faulty one is switched on at t=0.1s and HIF occurs between t=0.95s and t= 1.6s. It can be seen that when the faulty feeder is switched on there is also a transient in the sound feeder. A magnification of the transient resultant from switching on the faulty feeder is shown on a picture-in-picture of Fig. 4a. Small load switching on and off does not generally make *HIF alarm signal* go positive. Very strong transients occur at the beginning and end of HIF and between them *HIF alarm signal* stays positive. The first transient in Fig. 4b results from the simulation startup when all feeders are switched on.

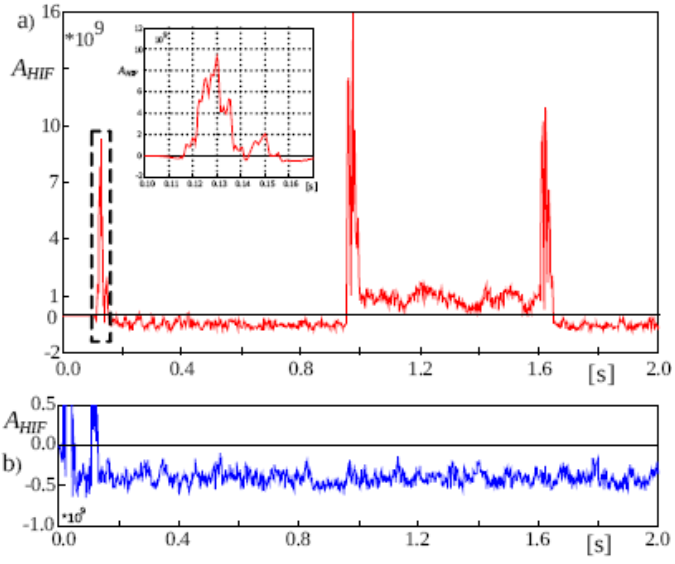

Fig. 4. HIF alarm signals A_{HIF}, in case of switching heavily loaded feeder 5 and HIF, measured in faulted feeder 5—a) and sound feeder 4—b)

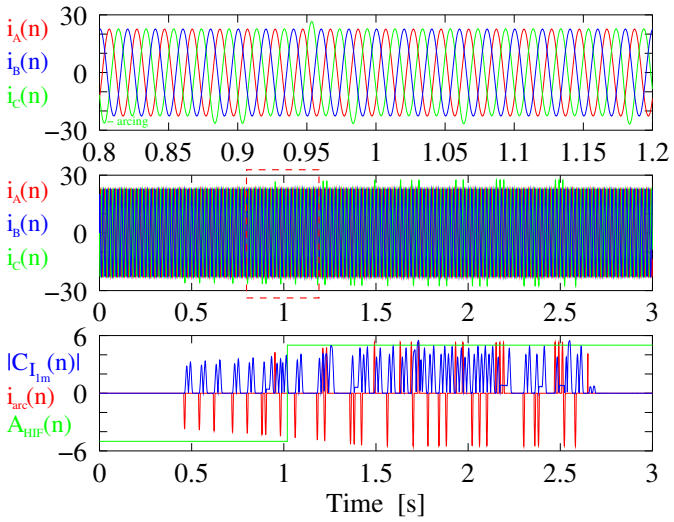

Fig. 5. Sparking high impedance fault detecion results, case 1

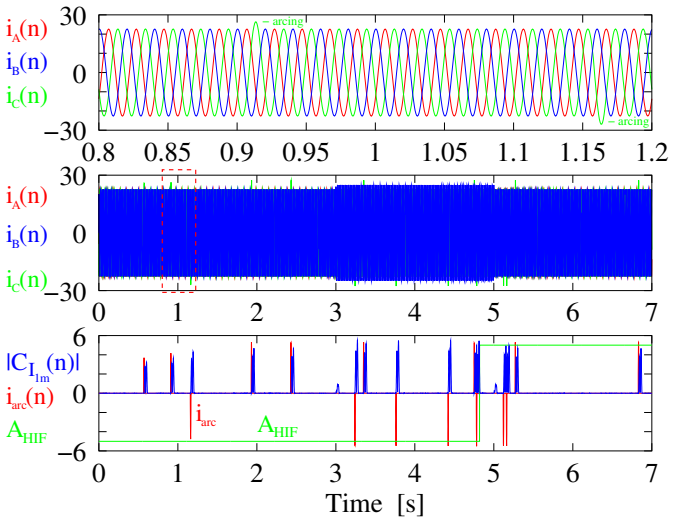

Fig. 6. Sparking high impedance fault detecion results, case 2

G. HIF Detection Scheme Evaluation

The simulation research which was performed using fault signals generated in MV system model described in appendix proves the correct operation of presented HIF detection scheme. Selected results of high impedance sparking faults detection are presented in Fig. 4 – 6. In the first case, a sparking fault is considered in lightly loaded feeder. Phase currents measured during the fault are depicted in Fig.5b where some random arcing between $t = 0.4s$ and $t = 2.7s$ can be observed. It is an initial stage of a HIF, which developes into a permament fault later on. To increase the readibility of Fig. 5b a small fraction of it was enlarged in Fig. 5a where it can be seen that random arcing introduces only small changes of a phase current waveform. Fault detection results are shown in Fig. 5c which pictures filtered arcing signal $i_{arc}(n)$, *HIF 3D criterion quantity signal* $|C_{I_{1m}}(n)|$ and *HIF alarm signal*. As can be seen each flash-over is acompanied with transient of *HIF 3D criterion quantity signal* $|C_{I_{1m}}(n)|$. The high impedance sparking fault is detected as a result of flash-overs sequence which makes *HIF alarm signal* positive during a period longer than the safety margin delay set to $0.06s$ after about $\Delta t = 0.6s$ since the occurrence of the first flash-over.

In the second case, another sparking fault is considered together with switching on and off some load between $t = 3s$ and $t = 5s$ of the simulation. The probability of firing an arc was chosen much lower than in the first case. Phase currents during the fault are presented in Fig. 6b and in bigger scale in Fig. 6a. Fault detection results are shown in Fig. 6c in the same manner as in former case. As can be seen again each flash-over is acompanied with transient of *HIF 3D criterion quantity signal* $|C_{I_{1m}}(n)|$. The high impedance sparking fault is detected when counted number of random flash-overs exceeds *a sparking fault count limit* which was set to 10. It can be seen from that example that load switching on and off operationals do not affect the HIF detection process.

In presented examples HIFs with small arc currents were chosen to stress out the algorithm's big sensitivity. A phase signal disturbance level limits it from the bottom and also contributes to threshold polynomial (20) coefficients a_k values. The disturbance level strongly affects *the criterion quantity signal algorithm* which contains a differential module for computing *a current perpendicular-to detail vector according* to (15). As white noise might be perceived by the criterion quantity determining algorithm as a low magnitude arc current it pumps up values of *the criterion quantity signal*. After all as background noises have different characteristics than arc currents the later can be still identified.

IV. Conclusion

Presented in the paper a new 3DPPS approach to power protection problem solutions is supposed to be an alternative to currently used standard methods.

The algorithm which has been described in this paper works very efficiently in grounded power systems producing very reliable criterion quantity $|C_{I_{1m}}(n)|$ signal. Because big loads switching on or off can result in *HIF 3D alarm signal* positive overshooting of hard to predict magnitude and this transient is short *the safety margin delay* was introduced to differentiate that kind of transients and real HIF occurrences.

The algorithm, thanks to newly developed 3D methodology, can detect very low arc current when sparking high impedance fault occurs in a pretty strongly contaminated feeder. The HIF detection sensitivity depends on currents disturbance level (white noise component content). The algorithm can also signal out any kind of short-circuit current which flows via the measurement point.

Appendix
Model of a System

The model of MV system used for generating current and voltage signals is shown in Fig. 7a. It was modeled with ATPDraw/EMTP software. Upstream network is represented

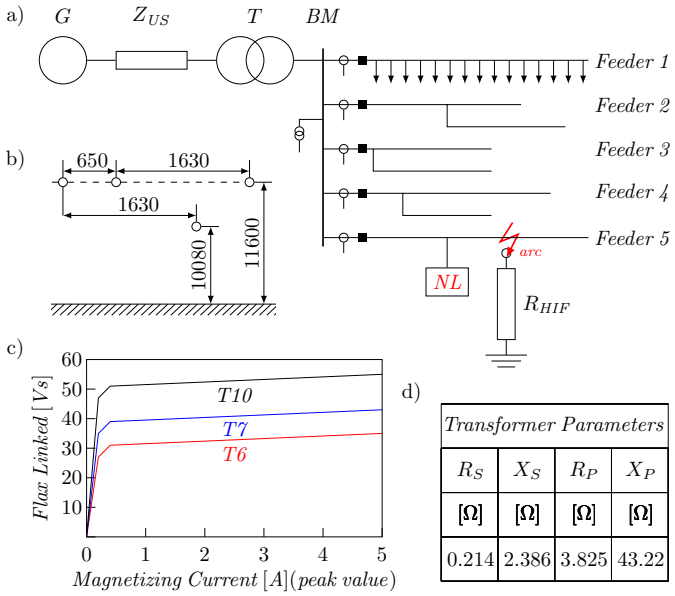

Transformer Parameters			
R_S	X_S	R_P	X_P
[Ω]	[Ω]	[Ω]	[Ω]
0.214	2.386	3.825	43.22

Fig. 7. One line diagram of the test model a), geometrical data for feeder wires configuration (all dimensions in [mm]) b), magnetizing characteristics of a transformer core c) and transformer leakage impedance parameters d)

by a voltage source behind an equivalent impedance $Z_1 = 0.06 + 6.049\Omega$ and $Z_0 = 0.09 + 9.074\Omega$. It is connected with MV lines via transformer Tr (Yg/yg $66kV/15kV$, parameters in a table in Fig. 7d). There are three cases considered with different magnetizing characteristics of the transformer core, Fig. 7b, in order to verify the proposed algorithm against current and voltage signals with different harmonic content. MV asymmetric overhead lines presented in Fig. 7c were modeled with LCC and have lengths $50m$ and $75m$ in different feeders. MV/LV transformers and loads are modeled *RLg* circuits of powers $S_n = 07.5 - 7.5MVA$, $\cos\varphi = 0.9 - 0.96$ were generated to get an unbalance of phase components of Z_{RL} up to $\pm 20\%$. In every feeder there are connected two 3 phase noising loads *NL* which initial resistance of each is $2k\Omega$ and it changes in a random manner in time and value during a simulation (there is only one *NL* in feeder 5 indicated in Fig. 7a). Electric arc model was implemented after [3] in MODELS part of ATP/EMTP, eq. (2) and (3) are solved at every simulation step. To obtain sparking faults a probability coefficient was introduced to determine if arc should burn in a given half-period of a signal or not. Signal measurements are performed on secondary side of instrumental transformers, at bus *BM*, at the output of second order *RC* low-pass analogue filters, which are also used as an antialiasing filters with a cut-off frequency set to $f_B = 350Hz$. There are also white noise signals in phase current signals added on the secondary side of instrument transformers before analogue filtering. It is assumed that white noise magnitude is of a level of 1% of the heaviest feeder load. The HIF detection algorithm itself was implemented in MODELS.

ACKNOWLEDGMENT

This work was supported by the 2nd Brain Korea 21 Project.

REFERENCES

[1] J. Carr, "Detection of high impedance faults on multi-grounded primary distribution systems," IEEE Trans. on Power Apparatus and Systems, vol. PAS-100, no. 4, pp. 2008-2016, Apr. 1981.

[2] H. Calhoun, M.T. Bishop, C.H. Eichler and R.E. Lee, "Development and testing of an electro-mechanical relay to detect fallen distribution conductors," IEEE Trans. on Power Apparatus and System, vol. PAS.-101, no. 6 , pp. 1643-1650, June 1982.

[3] M.M. Michalik, W. Rebizant, M. Lukowicz, S.-J. Lee and S.-H. Kang, "High-Impedance Fault Detection in Distribution Networks with Use of Wavelet-Based Algorithm," IIEEE Transactions on Power Delivery, Vol. 21, No. 4, Oct. 2006, pp. 1793-1802.

[4] X. Dong, T. Cui, A. Juszczyk, "A novel directional earth fault detection scheme based on residual current," 5th Myongji University-Tsingua University Joint Seminar on Protection & Automation, Oct. 29-30 2008.

[5] M.M. Michalik, W. Rebizant, M. Lukowicz, S.-J. Lee and S.-H. Kang, "New ANN-based algorithms for detection HIF im multigrounded MV networks," IEEE Trans. on Power Delivery, vol. 23, no. 1, pp. 58-66,Jan. 2008.

[6] W.H. Kwon, G.W. Lee, Y.M. Park, M.C. Yoon and M.H. Yoo "High Impedance Fault Detection Utilizing Incremental Variance of Normalized Even Order Harmonic Power," IEEE Trans. on Power Delivery, vol. 6, no. 2, Apr. 1991.

[7] C.-J. Kim and B.D. Russel, "Harmonic beraviour during arcing faults on power distribution feeders," Electric Power System Research, vol. 14, pp. 219-225, 1988.

[8] A.E. Emanuel and E.M. Gulachenski, "High impedance fault arcing on sandy soil in 15 kV distribution feeders: Contribution to the evaluation of the low frequency spectrum," IEEE Trans. on Power Delivery. vol, 5, no. 2, Apr. 1991.

[9] A.A. Girgis, W. Chang and E.B. Makram, "Analysis of high impedance fault generated signals using a Kalman filtering approach," IEEE Trans. on Power Delivery, vol. 5, no. 4, pp. 1714-1724, Nov. 1990.

[10] P.R. Sliva, A. Santos Jr. and F.G Jota, "An intelligent system for automaqtic detection of high impedance faults in electrical distribution systems," Proceedings of the 38th Midwest Symposium on Circuits and Systems, vol. 1,

[11] D. Bak, S.–J. Lee, S.–H. Kang, M.–S. Choi, W. Rebizant, "3D protection scheme proposal for HIF detection criterion quantity presentation," 5th Myongji University-Tsingua University Joint Seminar on Protection & Automation, Oct. 29-30 2008.

[12] D. Bak, S.–J. Lee, S.–H. Kang, M.–S. Choi, W. Rebizant, "New Approach to Arcing High Impedance Faults Detection in Medium Voltage Distribution Network," Proceedings of APAP2010, Jeju, Oct. 2009.